JOURNAL OF VIROLOGY, Jan. 1998, p. 527–534 Vol. 72, No. 1
0022-538X/98/$04.00+0

The Coronavirus Transmissible Gastroenteritis Virus Causes Infection after Receptor-Mediated Endocytosis and Acid-Dependent Fusion with an Intracellular Compartment

G. H. HANSEN,[1] B. DELMAS,[2] L. BESNARDEAU,[2] L. K. VOGEL,[1] H. LAUDE,[2] H. SJÖSTRÖM,[1] AND O. NORÉN[1]*

Biochemistry Laboratory C, Department of Medical Biochemistry and Genetics, The Panum Institute, DK-2200 Copenhagen N, Denmark,[1] and Unité de Virologie Immunologie Moléculaires, INRA, F-78350 Jouy-en-Josas, France[2]

Received 21 May 1997/Accepted 18 September 1997

Aminopeptidase N is a species-specific receptor for transmissible gastroenteritis virus (TGEV), which infects piglets, and for the 229E virus, which infects humans. It is not known whether these coronaviruses are endocytosed before fusion with a membrane of the target cell, causing a productive infection, or whether they fuse directly with the plasma membrane. We have studied the interaction between TGEV and a cell line (MDCK) stably expressing recombinant pig aminopeptidase N (pAPN). By electron microscopy and flow cytometry, TGEV was found to be associated with the plasma membrane after adsorption to the pAPN-MDCK cells. TGEV was also observed in endocytic pits and apical vesicles after 3 to 10 min of incubation at 38°C. The number of pits and apical vesicles was increased by the TGEV incubation, indicating an increase in endocytosis. After 10 min of incubation, a distinct TGEV-pAPN-containing population of large intracellular vesicles, morphologically compatible with endosomes, was found. A higher density of pAPN receptors was observed in the pits beneath the virus particles than in the surrounding plasma membrane, indicating that TGEV recruits pAPN receptors before endocytosis. Ammonium chloride and bafilomycin A_1 markedly inhibited the TGEV infection as judged from virus production and protein biosynthesis analyses but did so only when added early in the course of the infection, i.e., about 1 h after the start of endocytosis. Together our results point to an acid intracellular compartment as the site of fusion for TGEV.

Coronaviruses cause a wide spectrum of diseases in humans and animals, among which respiratory and enteric diseases are the most commonly seen (for a review, see reference 19). Epithelial cells of the digestive and respiratory tracts are the primary sites of replication for many coronaviruses. It is of great interest to understand in detail how different genetic subsets of coronaviruses (11) gain entry into these cells and whether they use similar or different strategies for fusion and penetration. Substantial evidence has been provided that coronaviruses enter their target cells by using different plasma membrane glycoproteins as receptors. Thus, several members of a family of carcinoembryonic antigens are known to act as receptors for mouse hepatitis virus (MHV) (12, 43). The class II membrane protein aminopeptidase N (APN) (26, 31) was demonstrated to be the major receptor for the porcine coronavirus transmissible gastroenteritis virus (TGEV) (8), the human coronavirus 229E (42), the feline coronavirus (2, 38), and the canine coronavirus (2, 38), all of which belong to a genetic subset that differs from that of MHV (11). APN is apically expressed in epithelial cells, which has the consequence that these cells are preferably infected from the apical side (34). Studies on the biosynthesis and intracellular transport of human APN in MDCK cells have shown that the majority of the APN is transported directly from the trans-Golgi network to the apical membrane (41).

The S glycoprotein of the coronavirus envelope plays a crucial role in the early steps of infection, since it carries functions for both receptor binding (15, 23, 25) and virus-cell membrane fusion (6). A complete understanding of the infection mechanisms of the coronaviruses includes the identification of their site of fusion. It is an unsettled matter whether penetration occurs by fusion directly with the plasma membrane or whether the different coronaviruses are endocytosed before fusion and penetration (19, 28). Until now most of the studies aimed at answering this question have focused on MHV. It has been shown that low pH is not a requirement for MHV infection (13, 21). In addition, it has been reported that MHV internalization by endocytosis does not necessarily lead to a productive infection (1, 21). Furthermore, the pH optimum for the cell-cell fusion activity of MHV is above 7.0 (35, 37). Taken together, these data make it most likely that fusion and penetration of MHV take place at the plasma membrane level. On the other hand, it has been reported that MHV infection is delayed by ammonium chloride (29), which is known to prevent pH-dependent membrane fusion in other virus systems (27, 28). This might suggest that endocytosis of MHV occurs prior to penetration (22, 29). However, the observed retardation by ammonium chloride could as well depend on unspecific cellular effects of the drug.

We have studied the early virus-cell interactions of TGEV in order to settle whether this virus fuses with intracellular membranes after endocytosis of the TGEV-pig APN (TGEV-pAPN) complex or whether fusion occurs directly after attachment to the primary receptor at the cell surface. For this purpose we used a transfected cell clone (pAPN-MDCK) of the polarized cell line MDCK which stably expresses recombinant wild-type pAPN at high levels (8). This makes it possible to monitor the TGEV-pAPN complexes and pAPN alone by immunoelectron microscopy. For some experiments analyzing the importance of low endosomal pH for infection, the naturally fully permissive ST cells (24) were used as well. A direct

* Corresponding author. Mailing address: IMBG, Biochemistry Laboratory C, The Panum Institute, Blegdamsvej 3, DK-2200 Copenhagen N, Denmark. Phone: 45 3532 7793. Fax: 45 3536 7980. E-mail: noren@biobase.dk.

interaction between the TGEV receptor pAPN and TGEV at the plasma membrane level was demonstrated, and the formation of this complex was found to increase endocytosis. After endocytosis, the TGEV-pAPN complexes were transported further to large intracellular vesicles that were morphologically compatible with endosomes. Bafilomycin A_1 and ammonium chloride added before endocytosis inhibited infection in pAPN-MDCK cells and inhibited productive infection in ST cells, demonstrating that acidity is important for infection. These findings provide biochemical evidence that the morphological observations of endocytosis are related to the productive infection.

MATERIALS AND METHODS

Virus and cells. The cell-adapted Purdue-115 strain was used as a TGEV source. Virus suspensions were produced on the PD5 cell line, purified by centrifugation through a sucrose gradient (purified virus particle suspension, 1.2 mg/ml), and then titrated on the ST cell line as described earlier (24) (physical/infectious particle ratio, 10 to 50) (23a). pAPN-MDCK cells (8) or transfected MDCK cells expressing tailless pAPN (TLpAPN-MDCK cells) (see below) were grown in Eagle's minimal essential medium supplemented with 2 mM L-glutamine, 10% fetal calf serum, 100 U of penicillin per ml, and 100 μg of streptomycin per ml.

Tailless pAPN cDNA, encoding a membrane-bound form of pAPN in which the 9-amino-acid N-terminal cytoplasmic sequence is exchanged for a Met-Ala-Arg sequence attached to the transmembrane part of the anchor, was constructed as previously described in detail (40). MDCK cells were transfected with 20 μg of pTej-4 (20), containing the cDNA coding for the tailless pAPN, and 2 μg of pSV2-neo. G418-resistant clones were then isolated and subcloned as described previously (40). The expression of tailless pAPN was analyzed by enzymatic measurements, and the correct molecular weight was assessed by sodium dodecyl sulfate (SDS) gel electrophoresis followed by Western blotting with a specific antibody directed against the denatured pAPN C subunit (36).

pAPN-MDCK or TLpAPN-MDCK cells (10^5) were seeded into 6.2-mm-diameter 24-well (0.45-μm-pore-size) Transwell chambers (Costar Europe Ltd., Badhoevedorp, The Netherlands). Twenty-four-hour-old confluent monolayers were used. The tightness of the filter-grown monolayers was assayed by filling the inner chamber to the brim and monitoring a constant fluid level after 5 h.

TGEV particles were adsorbed to tight filter-grown layers of pAPN-MDCK or TLpAPN-MDCK cells by adding 40 μl of purified virus particle suspension in 0.4 ml of medium (4°C) to the apical side (10^4 to 10^5 virus particles per cell). After adsorption (60 min, 4°C), the virus-containing solution was removed and the cells were rinsed once and further incubated at 38°C for different lengths of time (0 to 60 min). The incubations were stopped by cooling to 4°C, and the filters were then washed three times with isotonic phosphate-buffered saline, pH 7.2.

Inhibition of infectivity. Ammonium chloride and bafilomycin A_1 (Sigma Chemical Co., St. Louis, Mo.) (3), both of which are known to neutralize low-pH organelles, were used as inhibitors of virus penetration.

TGEV (50 PFU per well) was added to pAPN-MDCK cell monolayers in minimal essential medium containing newborn calf serum (5%). After 120 min at 4°C, unbound virus particles were removed by rinsing with the medium three times. Ammonium chloride (25 mM final concentration) was then added to the incubation mixtures at different time points before and after the temperature was raised to 38°C (see Fig. 5). In all experiments the cells were left with ammonium chloride for 2 h. The cells were then washed free of the drug with minimal essential MEM medium. The perturbation of productive infection was measured as a reduction of the cytopathic effect on the cells. The cytopathic effect was measured as the reduction of the acetic acid-mediated release of crystal violet incorporated in cells surviving the cytopathic effect of TGEV after fixation and staining, as previously described in detail (9). Similar experiments were also performed with ST cells and 200 PFU per well, and the degree of perturbation was assayed by the reduction in plaque formation (24).

To further study the importance of organelle acidity for TGEV infection, the effects of bafilomycin A_1 and ammonium chloride on the biosynthesis of viral proteins was studied by using the naturally permissive ST cells (24). TGEV was adsorbed and endocytosis was initiated as described above for the pAPN-MDCK cells. Bafilomycin A_1 (5 μM) or ammonium chloride (25 mM) was added at different times (0 to 180 min) after the start of endocytosis. Three hours after virus adsorption, the cultures were supplemented with 50 μCi of [^{35}S]methionine per ml of medium and then incubated for 5 h for protein labelling. The cells were then solubilized by incubation (1 h, 4°C) in 10 mM Tris-HCl (pH 8.0) containing 2% Triton X-100, 0.15 M NaCl, 0.6 M KCl, and 0.5 mM $MgCl_2$, and 10^3 U of aprotinin per ml was added. Undissolved material was removed by centrifugation (10,000 × *g*, 30 min, 4°C). TGEV proteins were immunoisolated and analyzed by SDS-polyacrylamide gel electrophoresis as described earlier (33).

Flow cytometry. pAPN- and human APN-expressing MDCK cells were released from the culture bottles by trypsination. The cells (5×10^5) were incubated at 4°C for 1 h in the presence of TGEV (2×10^8 PFU/ml). After being washed three times with cold staining medium (Dulbecco's modified Eagle's medium supplemented with 3% bovine serum albumin and 0.02% sodium azide), the cells were incubated (4°C, 1 h) in TGEV antibody solution produced in pigs (24) (diluted 500 times). The washed cells were then incubated in an excess of fluorescein isothiocyanate-labelled affinity-purified rabbit immunoglobulin G (IgG) against porcine IgG (Biosys, Compiègne, France). The cells were then washed, fixed in phosphate-buffered paraformaldehyde (5%), and analyzed on a FACScan apparatus (Becton Dickinson).

Ultrastructural analyses. The cells were fixed in 2.5% glutaraldehyde in 0.1 M phosphate buffer, pH 7.2 (PB), for 30 min. After fixation, the filters were cut from their holders, washed in PB, and postfixed in 1% osmium tetroxide in PB for 15 min at 4°C. After treatment with 1% uranyl acetate in water for 1 h at 20°C, the cells were dehydrated in a graded series of ethanol solutions and finally embedded in Epon. Ultrathin sections were cut on an Ultramicrotome III (LKB, Stockholm, Sweden), stained in lead citrate for 5 s, and examined in a Zeiss EM 900 electron microscope operated at 80 kV. Apical vesicles were counted as the vesicles present in the 20% apical part of the cells.

Immunogold staining. Immunogold labelling of pAPN was performed on filter-grown cells fixed and processed as described above. Ultrathin sections (approximately 100 nm) were etched in 1% hydrogen peroxide in water for 5 min and washed in TBS (0.05 M Tris-HCl buffer, 0.15 M NaCl, pH 7.4) containing 1% Triton X-100. To minimize nonspecific antibody adsorption, the sections were treated with 3% bovine serum albumin in gold buffer (0.02 M Tris-HCl, 0.15 M NaCl, 0.25% bovine serum albumin, and 1% Triton X-100, pH 8.2) for 30 min at 20°C. The sections were then incubated in a rabbit anti-pAPN IgG (diluted in gold buffer) directed against the denatured pAPN C subunit (36) for 20 h at 4°C and for 1 h at 20°C in a moist chamber. After three washes (10 min each) in gold buffer, the sections were incubated with centrifuged (5,000 rpm, 15 min; SS-34 Sorvall centrifuge) sheep anti-rabbit IgG conjugated to 5-nm-diameter gold particles (16) for 30 min at room temperature. The sections were rinsed three times (10 min each) in gold buffer, twice (5 min each) in TBS, and twice (5 min each) in water. The sections were finally contrasted in lead citrate for 45 s before examination in a Zeiss EM 900 electron microscope operated at 80 kV.

The quantitative evaluation of the density of pAPN in the plasma membrane beneath the virus particles and in the adjacent plasma membrane was performed directly on a monitor connected to the electron microscope. The numbers of gold particles in the formed pits beneath the virus particles and in a corresponding length of the adjacent plasma membrane were counted.

Statistics. Quantitative data are presented as means ± standard errors. For significance tests, Student's *t* test was used.

RESULTS

TGEV is endocytosed and transported to large vesicles in the target cells. pAPN-MDCK cells, which express pAPN at a high level, were incubated with TGEV at 4°C for 60 min from the apical side, followed by incubation at 38°C for different lengths of time (0 to 60 min). The cells were directly fixed at the end of the incubation and further processed for electron microscopy, and the morphology was examined.

Initially a high number of virus particles were seen closely associated to the apical plasma membrane (Fig. 1A). Frequently the virus particles were seen in close proximity to pits (Fig. 1B and C) formed by invagination of a thickened plasma membrane, indicating that the pits are protein coated. Infection of pAPN-MDCK cells with TGEV induced a significant ($P \geq 0.98$) increase of the number of pits observed per cell profile in comparison to that in uninfected cells (Table 1). Similarly a significant ($P \geq 0.95$) increase in the number of pits was observed when TLpAPN-MDCK cells were used in a similar experiment (Table 1).

Approximately 20-nm-wide gaps between the plasma membrane of the coated pits and the viral membrane were observed (Fig. 1B and C). Frequently, electron-dense linear structures were observed in these gaps. This material most probably represents the viral spikes formed by S-protein trimers (7) interacting with their membrane receptors (pAPN). We have not observed any continuity between viral and plasma membranes, which is compatible with the view that fusion does not occur at the plasma membrane level.

After 10 min of incubation at 38°C, the apical cell surface was partially cleared from viral particles. TGEV particles were now present in small vesicles beneath the apical plasma membrane, as illustrated by the electron micrographs in Fig. 1D and

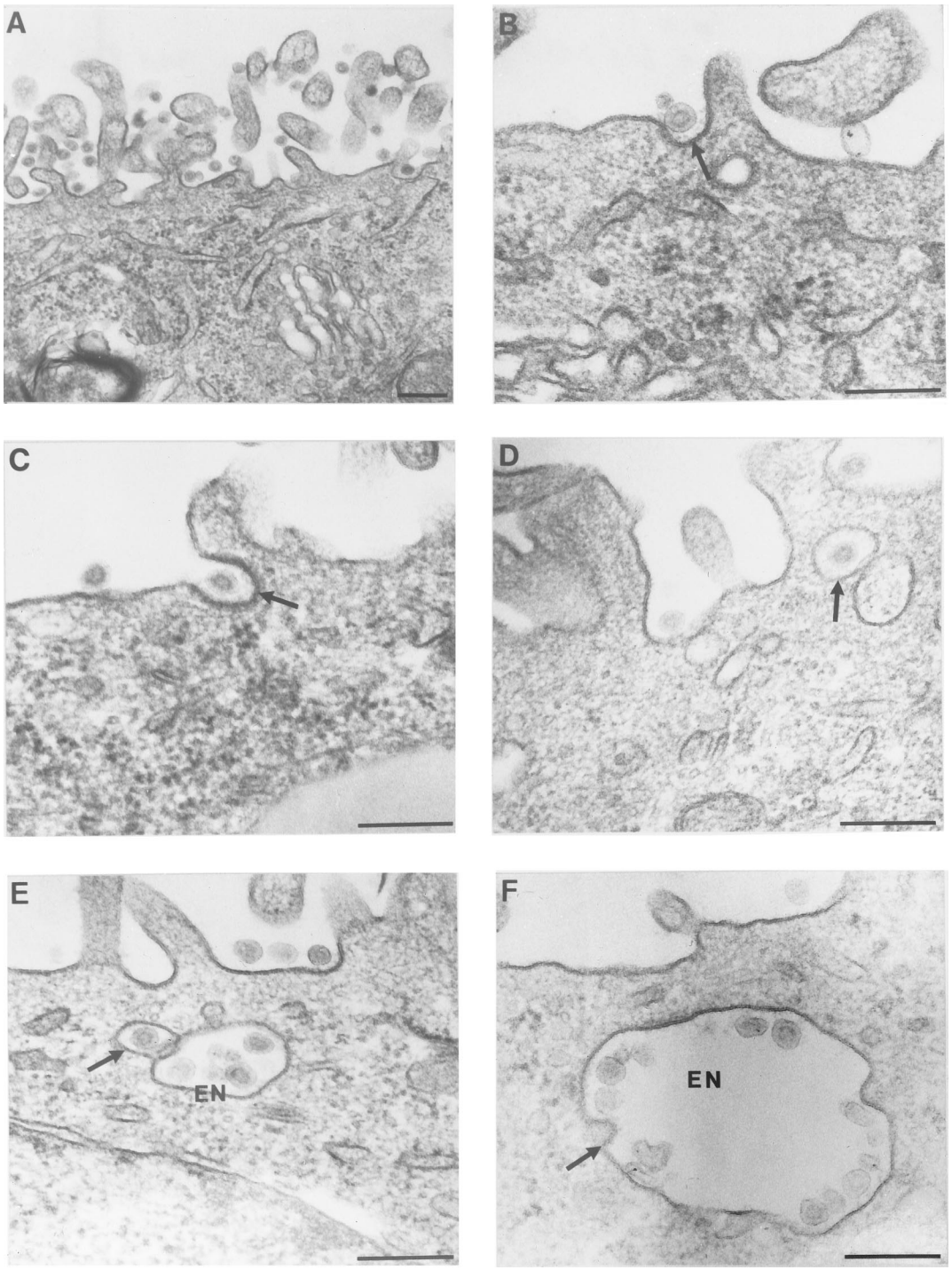

FIG. 1. Apical binding and endocytosis of TGEV by pAPN-MDCK cells. (A) A large number of TGEV particles are seen in close proximity to the apical membrane after initial adsorption (60 min, 4°C) and incubation at 38°C (3 min). (B and C) TGEV particles (arrows) are seen in pits with a thickened plasma membrane after adsorption and incubation at 38°C for 3 min. (D) TGEV particle in a smooth apical vesicle (arrow) after incubation at 38°C for 10 min. (E) The arrow points to a smooth transport vesicle containing a TGEV particle which is positioned close to a larger endosome-like vesicle (EN), indicating vesicle fusion. (F) TGEV particles in large intracellular vesicles after incubation at 38°C for 30 min. The arrow indicates putative continuity between viral and vesicle membranes, indicating fusion between the TGEV particle and the intracellular vesicle. Bars, 200 nm.

E. Thus, 0.64 ± 0.08 (n = 150) apical vesicles per cell profile were found in the TGEV-infected cells 10 min after the elevation of the temperature to 38°C. This is a significantly ($P \geq 0.99$) higher value than that found for uninfected cells (0.36 ± 0.05; n = 150). Occasionally, TGEV-containing smooth vesicles were observed close to large vesicles (Fig. 1E), indicating fusion between these compartments. Large intracellular vesicles (Fig. 1F) containing many TGEV particles were often

TABLE 1. Number of pits in TGEV-infected and uninfected pAPN-MDCK and TLpAPN-MDCK cells[a]

Cell type	No. of pits per cell profile (SE)	No. of profiles
pAPN-MDCK		
TGEV infected	1.83 (0.16)	80
Uninfected	0.43 (0.08)	68
TLpAPN-MDCK		
TGEV infected	0.73 (0.11)	136
Uninfected	0.46 (0.08)	70

[a] The number of pits on each cell profile seen in the electron microscope at 10 min (pAPN-MDCK cells) or 30 min (TLpAPN-MDCK cells) postadsorption was counted.

observed. In these large vesicles the virus particles were seen associated with the cisternal face of the membrane at a distance of approximately 20 nm. The electron-dense material between the TGEV particles and the membrane, which is assumed to represent the S-protein–pAPN complex, was also observed in these vesicles. Morphologically, these vesicles are compatible with endosomes. Free, non-membrane-associated virus particles were very infrequently observed. The TGEV-pAPN complexes are thus also kept intact in these endosome-like structures, which are likely to have an acidic pH promoting the dissociation of the ligand-receptor complexes (5).

pAPN is specifically involved in TGEV-cell binding and in the internalization process. Flow cytometry shows that binding of TGEV to the cell surface is specifically dependent on the presence of pAPN. This is demonstrated by an analysis using the pAPN-MDCK cells and MDCK cells transfected by human APN (39). Distinct TGEV binding was seen for the pAPN-MDCK cells (Fig. 2b), but no such binding was observed for the MDCK cells transfected with human APN (Fig. 2a).

Immunogold labelling of pAPN on the TGEV-infected pAPN-MDCK cells was seen in close proximity to the virions present in pits (Fig. 3A and B) after incubation at 38°C for 10 min after the viral adsorption. In the pits beneath the virus particles, 2.18 ± 0.14 (n = 348) gold particles were observed. This is significantly higher ($P \geq 0.999$) than the number (0.73 ± 0.08; n = 347) found in corresponding lengths of the plasma membrane outside the pits in the same cell. The corresponding values for TGEV-infected TLpAPN-MDCK cells are 2.8 ± 0.19 (n = 102) and 0.26 ± 0.05 (n = 101) in the corresponding lengths of the plasma membrane outside the pits, again showing a significant ($P \geq 0.999$) increase in labelling of the pits after TGEV infection. Together the data clearly demonstrate that the interaction between TGEV and its receptor pAPN causes a clustering of pAPN molecules.

In the pAPN-MDCK cells, two distinct populations of large intracellular vesicles were observed. One population carries TGEV particles; another does not. The population containing TGEV particles displayed a significantly higher ($P \geq 0.999$) gold labelling (12.27 ± 0.96 gold particles per organelle [64 organelles analyzed]) than the vesicles that are free of TGEV (1.11 ± 0.21 gold particles per organelle [90 organelles analyzed]) (Fig. 3C and 4), showing that the majority of pAPN is present in the same organelles as the endocytosed TGEV.

TGEV membrane fusion and penetration occur in an acidic compartment. Biochemical studies using the lysosomotropic drug ammonium chloride (30) or the proton pump inhibitor bafilomycin A_1 (3) showed that these drugs have a significant inhibitory effect on the TGEV infectivity. They completely blocked the effect of TGEV on ST cells and potently reduced the effect of TGEV on pAPN-MDCK cells when added during the first hour after the start of endocytosis. Ammonium chloride is known to raise the pH in intracellular organelles 1 min after addition (30), making it possible to inhibit a low-pH-dependent fusion process at defined time points. The almost complete inhibitory effect of ammonium chloride on the infectivity of TGEV in the fully permissive ST cells is demonstrated in Fig. 5b. Ammonium chloride does not influence the infectivity of TGEV later when present exclusively during the adsorption phase at 4°C, a temperature that blocks endocytosis. This indicates that the drug does not influence the binding of TGEV to the plasma membrane, as almost 100% infectivity is achieved after warming the system to 38°C, thereby allowing endocytosis.

Half-maximal inhibition occurred about 1 h after warming, suggesting that penetration occurs in late endosomes. Ammonium chloride also had a significant inhibitory effect on viral

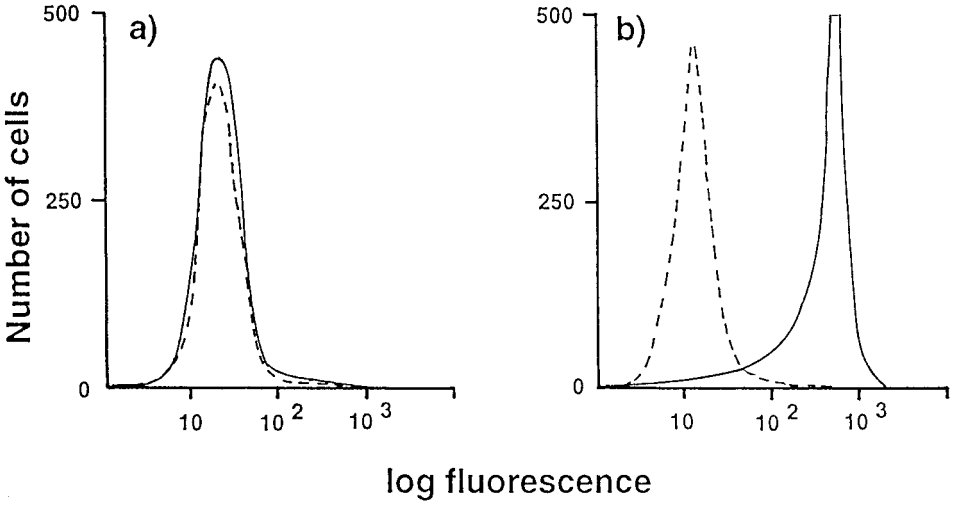

FIG. 2. Specific binding of TGEV to pAPN-MDCK cells. MDCK cells permanently expressing human APN (a) or pAPN-MDCK cells (b) were incubated with TGEV (solid lines) or mock incubated (dotted lines). Cellular binding of TGEV was monitored by flow cytometry after incubation with a porcine anti-TGEV serum followed by incubation with a fluorescein isothiocyanate-labelled rabbit IgG directed against porcine IgG.

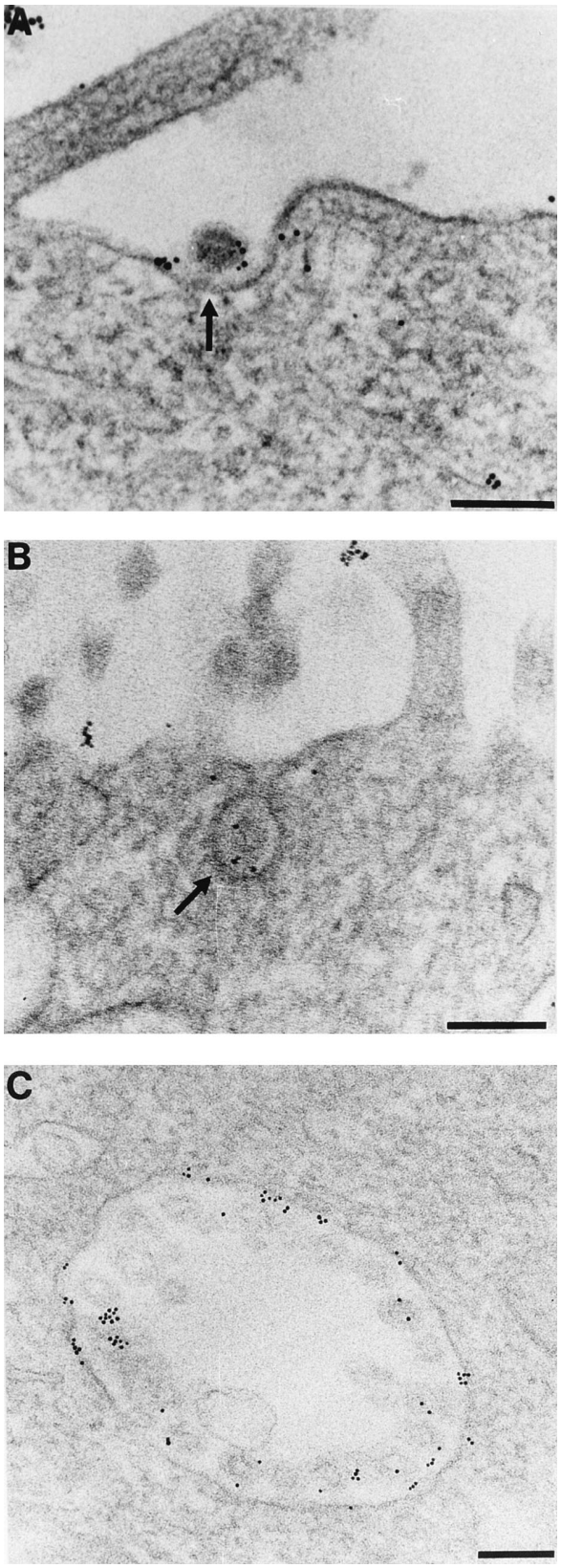

FIG. 3. Colocalization of pAPN and TGEV. Localization of pAPN was carried out by immunogold labelling of pAPN-MDCK cells which were incubated with TGEV from the apical side (4°C, 1 h). The cells were then incubated at 38°C for 10 min. (A) Gold labelling demonstrating the presence of pAPN is seen just beneath the TGEV particle (arrow) and to a lesser extent in the rest of the plasma membrane. (B) Gold labelling of a TGEV-containing pit (arrow), demonstrating colocalization between TGEV and pAPN. (C) Labelling of a large intracellular vesicle. The gold particles are seen all over the membrane localized to the cisternal side beneath the TGEV particles, demonstrating the presence of pAPN in close proximity to TGEV. Bars, 200 nm.

protein synthesis (Fig. 6B) when added 0 to 40 min after initiation of endocytosis.

A significant half-maximal inhibition of infection (Fig. 5a) was observed when similar experiments were carried out with the pAPN-MDCK cells. In this type of experiment, the drug effect was measured by an assay of reduction of cytopathic effect, as TGEV infection does not cause plaques in this cell system (9). In this case also, half-maximal inhibition occurred about 1 h after warming, supporting the idea that penetration occurs in late endosomes.

In addition, the proton pump inhibitor bafilomycin A_1 was used to further study the importance of acidic compartments for the TGEV infection. Addition of this drug at 0 to 40 min after adsorption of TGEV to ST cells strongly inhibited the TGEV infection as monitored by the complete inhibition of TGEV protein biosynthesis (Fig. 6A). The drug was without effect when added 80 min after adsorption or later, indicating that the sensitive period for viral inhibition is about 1 h after the start of viral uptake. This is compatible with the view that penetration occurs by a low-pH-dependent mechanism. Invaginations with a diameter similar to that of the membrane of the virus particles were occasionally observed in the TGEV-containing large vesicles (Fig. 1F). These invaginations may represent fusions between TGEV particles and the vesicular membranes, thus providing morphological support for the conclusion that fusion and penetration of TGEV occur in intracellular vesicles morphologically compatible with endosomes.

DISCUSSION

pAPN has been shown to be the major receptor for TGEV (8). In this study we extend this information by use of immunoelectron microscopy. Thus, we demonstrate that TGEV particles initially are adsorbed to the plasma membrane of the pAPN-MDCK cells via its receptor pAPN, as the immunogold labelling for pAPN is found in close proximity to the TGEV particles after virus binding. During binding, the virus particles carrying many receptor (pAPN) binding sites recruit pAPN molecules, as a local high density of pAPN molecules is observed beneath the virus particles. This phenomenon is not dependent on the cytoplasmic tail, as the tailless pAPN is concentrated in a similar way in the membrane. The formation of these pAPN-TGEV complexes in the plasma membrane seems to increase the endocytosis rate, as indicated by the increase in the number of pits and the number of apical vesicles in the infected cells. The virus particles seem to act as cross-linkers of pAPN, thereby inducing endocytosis in a way similar to that of antibodies against surface antigens (antibody-mediated endocytosis) (4). It is not known whether endocytosis of TGEV occurs via the clathrin- or non-clathrin-dependent mechanism or via the combination of both. The thickening of the membrane below the adsorbed TGEV particles observed in many cases might, however, indicate the involvement of clathrin-coated pits.

After endocytosis, the pAPN-TGEV complexes are transported to (or form) a distinct population of vesicles rich in TGEV particles and pAPN molecules. Morphologically, these vesicles are compatible with endosomes. The finding that neutralization of the acidic organelles, as demonstrated by the use

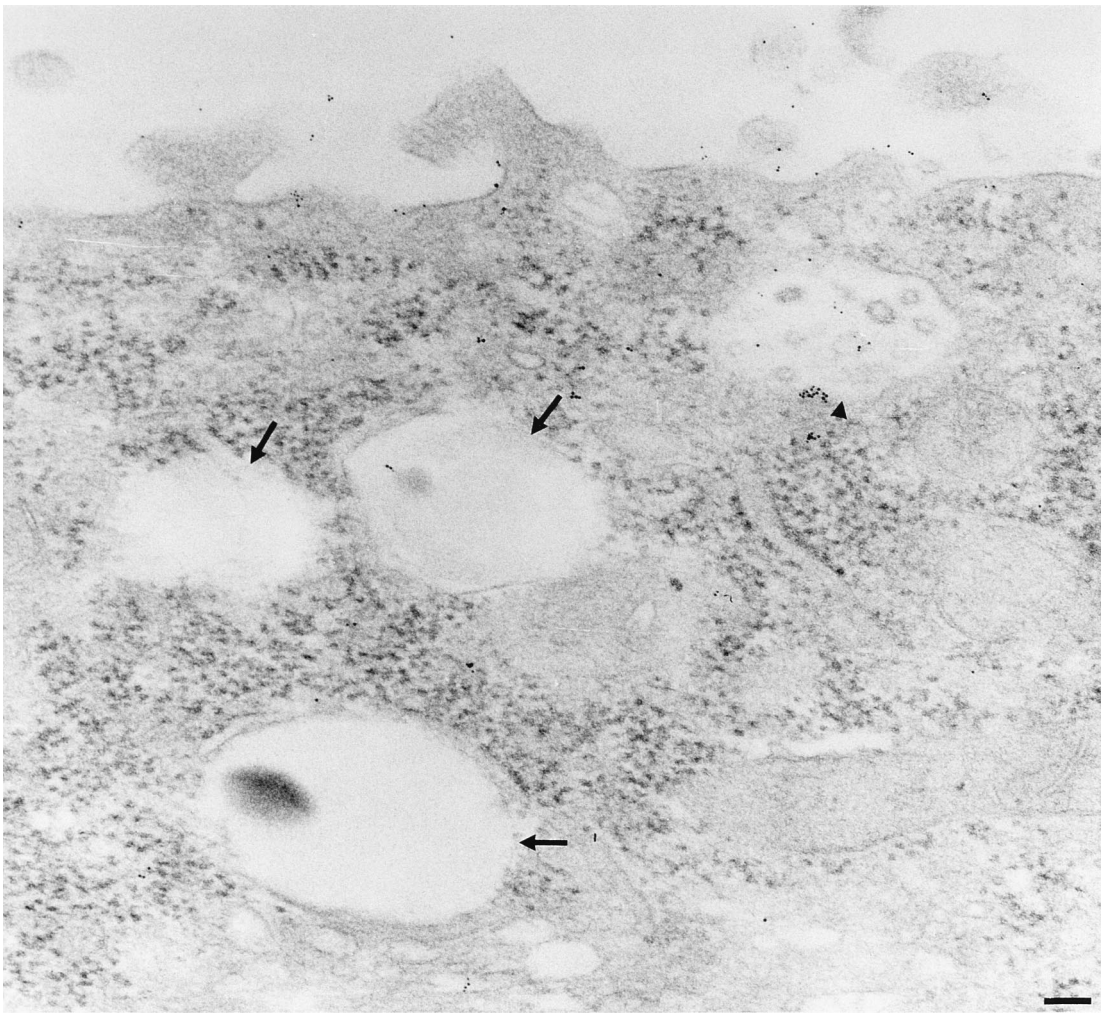

FIG. 4. TGEV- and pAPN-free large intracellular vesicles. The cells and labelling are as in Fig. 3. The arrows indicate vesicles free of TGEV particles and pAPN labelling. The arrowhead indicates a pAPN-TGEV-containing vesicle. Bar, 200 nm.

of ammonium chloride and bafilomycin A_1, has to occur not later than 1 h after initiation of endocytosis for a productive infection to occur suggests that a late endosomal population is the site for TGEV genome penetration. This notion is further supported by the electron microscopic observation of structures compatible with fusions between viral and the vesicular membranes. Thus, both morphological and biochemical data are compatible with the view that an intracellular vesicular compartment is the site of TGEV genome penetration. We never observed syncytium formation in any of the cell lines examined, even with a brief incubation of infected cells at a slightly acidic pH (unpublished data). This might argue against an acid mechanism for the virus-membrane fusion, thereby excluding an intracellular vesicular compartment like endosomes as the site of TGEV fusion and penetration. However, it is known that the requirements for syncytium formation are more stringent than those for fusion with membranes in target organelles (18). This weakens the importance of the absence of syncytium formation in the discussion of the site of viral fusion. TGEV is an enteropathogenic virus for which it is well established that natural infection in vivo is oronasal (32). Thus, exposure to the very low pH in the stomach does not lead to complete inactivation of the virus. TGEV infectivity has been shown to be unaltered down to pH 3 (24), which is an unusual feature among enveloped viruses. This could imply that a conformational change induced in the S protein is at least partially reversible, as has been described for the rabies virus (14). It might be suggested that exposure to acidic pH is not sufficient to induce and keep a putative fusion peptide in an exposed state but that an additional interaction with a membrane component, for example, the receptor (pAPN), is required.

In contrast to our observations for TGEV, syncytium formation has been observed for the mouse coronavirus MHV. In this case a slightly alkaline pH has been found to be optimal for triggering MHV fusion (22, 35, 37). For this virus, internalization has been proposed to be of no importance for productive infection (1, 21). Thus, there seems to be a discrepancy between TGEV and MHV, which belong to two different genetic subsets of coronaviruses (11), with respect to site of fusion and penetration.

The mechanism for uptake and penetration of TGEV might also be of relevance for other coronaviruses of the same genetic subset, like human coronavirus 229E, which usually do not cause syncytium formation. The initial mechanism of infection for TGEV thus is very similar to what has been found for many other groups of enveloped viruses (18, 27, 28).

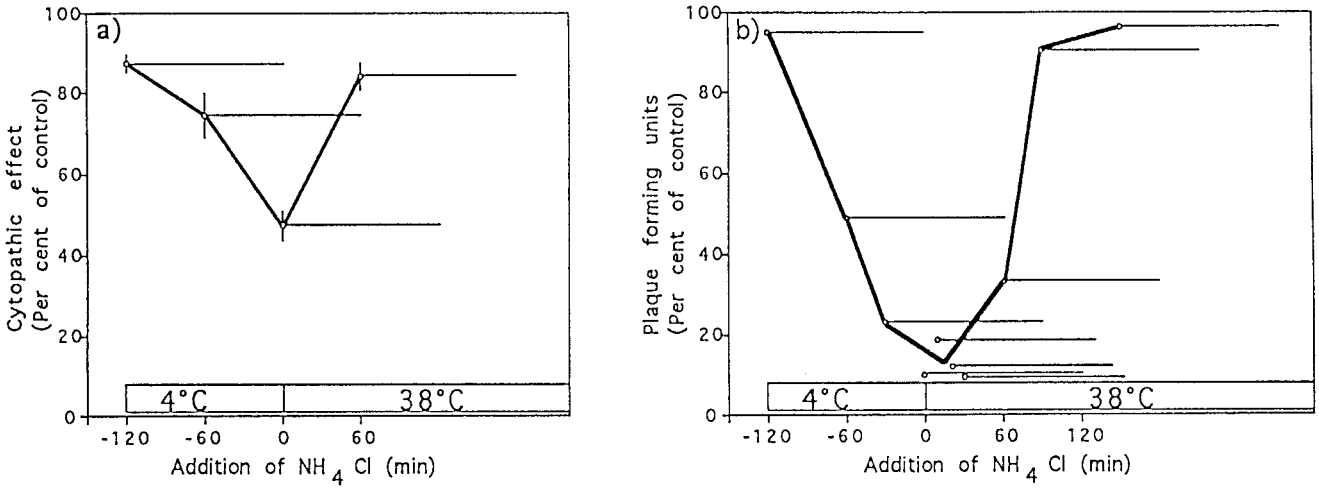

FIG. 5. Inhibitory effect of ammonium chloride on TGEV infectivity. Virions were bound to pAPN-MDCK cells (a) or ST cells (b) at 0°C for 120 min, and unbound virions were washed away. Ammonium chloride (25 mM final concentration) was added at the indicated times (○) and was present during different 2-h periods as indicated by the horizontal bars. The ammonium chloride was washed out of the cells at the ends of these periods. (a) The cytopathic effect was quantified colorimetrically by measuring cellular crystal violet association as described in Materials and Methods. The means and standard errors from three experiments are shown. (b) The cells were overlaid with agar at 38°C and incubated for 48 h at this temperature for plaque formation. The means from two different experiments are shown.

Together, the data reported in this paper strongly reinforce the opinion that pAPN is a functional receptor for TGEV. To our knowledge, our report is the first in which visualization of the cellular uptake of the virus-receptor complexes has been demonstrated. The model system presented in this paper constitutes a good system for further studies of the structural requirements of pAPN-TGEV interaction and the uptake of the virus-receptor complex. As a starting point for such studies, the binding site of TGEV has been mapped outside the catalytic site to the C-terminal part of pAPN (10). The identification of the structural parts of pAPN involved in endocytosis is of high interest for the understanding of the uptake mechanism. In this paper evidence is presented that pAPN-TGEV interaction stimulates endocytosis. How this is exerted is for the moment completely unknown. It might be speculated that the interaction stimulates protein kinase A-dependent phosphorylation, which has been demonstrated to increase endocytosis (17).

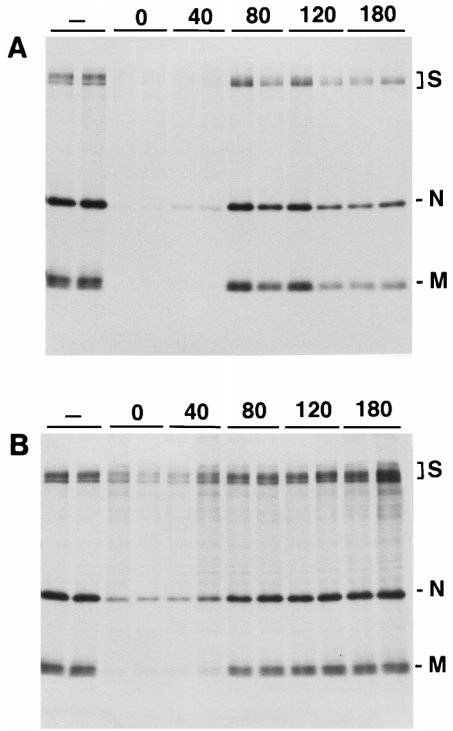

FIG. 6. Inhibitory effect of bafilomycin A_1 (a) and ammonium chloride (b) on TGEV infectivity. Virions were bound to ST cells at 0°C for 120 min, unbound virions were washed away with ice-cold medium, and then warm medium (37°C) was added. Bafilomycin A_1 (5 μM final concentration) (a) or ammonium chloride (25 mM) (b) was added at the indicated times (minutes) after adsorption. For each time, duplicate infections were performed. At 3 h after adsorption, [^{35}S]methionine was added. After 5 h of further incubation, the cells were solubilized and the viral proteins were immunoisolated, separated by SDS-polyacrylamide gel electrophoresis, and visualized by autoradiography.

ACKNOWLEDGMENTS

We thank L.-L. Niels-Christiansen, E. Thorsen, and J. Gelfi for skilful technical assistance.

We thank the Danish Cancer Society, the Danish Research Council of Health Sciences, and the Benzon Foundation for generous financial support. G.H.H., O.N., H.S., and L.K.V. were members of the Biomembrane Research Center, Aarhus University.

REFERENCES

1. **Asanaka, M., and M. C. Lai.** 1993. Cell fusion studies identified multiple cellular factors involved in mouse hepatitis virus entry. Virology **197:**732–741.
2. **Benbacer, L., E. Kut, L. Besnardeau, H. Laude, and B. Delmas.** 1997. Interspecies aminopeptidase N chimeras reveal species-specific receptor recognition by canine coronavirus, feline infectious peritonitis virus, and transmissble gastroenteritis virus. J. Virol. **71:**734–737.
3. **Bowman, E. J., A. Siebers, and K. Altendorf.** 1988. Bafilomycins: a class of inhibitors of membrane ATPases from microorganisms, animal cells, and plant cells. Proc. Natl. Acad. Sci. USA **85:**7972–7976.
4. **Bretscher, M. S.** 1984. Endocytosis: relation to capping and cell locomotion. Science **224:**681–686.
5. **Davis, C. G., J. L. Goldstein, T. C. Südhof, R. G. W. Anderson, D. W. Russell, and M. S. Brown.** 1987. Acid-dependent ligand dissociation and recycling of LDL receptor mediated by growth factor homology region. Nature **326:**760–765.
6. **De Groot, R., R. W. Van Leen, M. J. M. Dalderup, H. Vennema, M. C. Horzinek, and W. J. M. Spaan.** 1989. Stably expressed FIPV peplomer protein induces cell fusion and elicits neutralizing antibodies in mice. Virology **171:**493–502.
7. **Delmas, B., and H. Laude.** 1990. Assembly of coronavirus spike proteins into trimers and its role in epitope expression. J. Virol. **64:**5367–5375.

8. **Delmas, B., J. Gelfi, R. L'Haridon, L. K. Vogel, H. Sjöström, O. Norén, and H. Laude.** 1992. Aminopeptidase N is a major receptor for the enteropathogenic coronavirus TGEV. Nature **357:**417–419.
9. **Delmas, B., J. Gelfi, H. Sjöström, O. Norén, and H. Laude.** 1993. Further characterization of aminopeptidase N as a receptor for coronaviruses, p. 293–298. *In* H. Laude and J. F. Vautherot (ed.), Coronaviruses: molecular biology and virus-host interactions. Plenum Press, New York, N.Y.
10. **Delmas, B., J. Gelfi, E. Kut, H. Sjöström, O. Norén, and H. Laude.** 1994. Determinants essential for the transmissible gastroenteritis virus-receptor interaction reside within a domain of aminopeptidase N that is distinct from the enzymatic site. J. Virol. **68:**5216–5224.
11. **Duarte, M., J. Gelfi, P. Lambert, D. Rasschaert, and H. Laude.** 1993. Genome organization of porcine epidemic diarrhoea virus, p. 55–60. *In* H. Laude and J. F. Vautherot (ed.), Coronaviruses: molecular biology and virus-host interactions. Plenum Press, New York, N.Y.
12. **Dveksler, G. S., C. W. Dieffenbach, C. B. Cardellichio, K. McCuaig, M. N. Pensiero, G. S. Jiang, N. Beauchemin, and K. V. Holmes.** 1993. Several members of the mouse carcinoembryonic antigen-related glycoprotein family are functional receptors for the coronavirus mouse hepatitis virus A59. J. Virol. **67:**1–8.
13. **Gallagher, T., C. Escarmis, and M. J. Buchmeier.** 1991. Alteration of the pH dependence of coronavirus-induced fusion: effect of mutations in the spike glycoprotein. J. Virol. **65:**1916–1928.
14. **Gaudin, Y., C. Tuffereau, D. Segretain, M. Knossow, and A. Flamand.** 1991. Reversible conformational changes and fusion activity of rabies virus glycoprotein. J. Virol. **65:**4853–4859.
15. **Godet, M., J. Grosclaude, B. Delmas, and H. Laude.** 1994. Major receptor-binding and neutralization determinants are located within the same domain of the transmissible gastroenteritis virus (coronavirus) spike protein. J. Virol. **68:**8008–8016.
16. **Hansen, G. H., L.-L. Wetterberg, H. Sjöström, and O. Norén.** 1992. Immunogold labelling is a quantitative method as demonstrated by studies on aminopeptidase N in microvillar membrane vesicles. Histochem. J. **24:**132–136.
17. **Hansen, S. H., and J. E. Casanova.** 1994. Gs alpha stimulates transcytosis and apical secretion in MDCK cells through cAMP and protein kinase A. J. Cell Biol. **126:**677–687.
18. **Hernandez, L. D., L. R. Hoffman, T. G. Wolfsberg, and J. M. White.** 1996. Virus-cell and cell-cell fusion. Annu. Rev. Cell. Dev. Biol. **12:**627–661.
19. **Holmes, K. V., and M. C. Lai.** 1996. Coronaviridae: the viruses and their replication, p. 1075–1093. *In* N. Fields, D. M. Knipe, P. Howley, et al. (ed.), Fields virology, 3rd ed. Lippincott-Raven Publishers, Philadelphia, Pa.
20. **Johansen, T. E., M. S. Schøller, S. Tolstoy, and T. W. Schwartz.** 1990. Biosynthesis of peptide precursors and protease inhibitors using new constitutive and inducible eukaryotic expression vectors. FEBS Lett. **267:**289–294.
21. **Kooi, C., M. Cervin, and R. Anderson.** 1991. Differentiation of acid-pH dependent and non-dependent entry pathways for mouse hepatitis virus. Virology **180:**108–119.
22. **Krzystyniak, K., and J. M. Dupuy.** 1984. Entry of mouse hepatitis virus 3 into cells. J. Gen. Virol. **65:**227–231.
23. **Kubo, H., Y. Yamada, and F. Taguchi.** 1994. Localization of neutralizing epitopes and the receptor-binding site within the amino-terminal 330 amino acids of the murine coronavirus spike protein. J. Virol. **68:**5403–5410.

23a. **Laude, H.** Unpublished data.

24. **Laude, H., J. Gelfi, and J. M. Aynaud.** 1981. In vitro properties of low- and high-passage strains of transmissible gastroenteritis coronavirus of swine. Am. J. Vet. Res. **42:**447–449.
25. **Laude, H., J. M. Chapsal, J. Gelfi, S. Labiau, and J. Grosclaude.** 1986. Antigenic structure of transmissible gastroenteritis virus. I. Properties of monoclonal antibodies directed against virion proteins. J. Gen. Virol. **67:** 119–130.
26. **Look, T., R. A. Ashmun, L. H. Shapiro, and S. C. Peiper.** 1989. Human myeloid plasma membrane glycoprotein CD13 (gp150) is identical to aminopeptidase N. J. Clin. Invest. **83:**1299–1307.
27. **Marsh, M., and A. Helenius.** 1989. Virus entry into animal cells. Adv. Virus Res. **36:**107–151.
28. **Marsh, M., and A. Pelchen-Matthews.** 1994. The endocytic pathway and virus entry, p. 215–240. *In* E. Wimmer (ed.), Cellular receptors for animal viruses. Cold Spring Harbor Laboratory Press, Cold Spring Harbor, N.Y.
29. **Mizzen, L., A. Hilton, S. Cheley, and R. Anderson.** 1985. Attenuation of murine coronavirus infection by ammonium chloride. Virology **142:**378–388.
30. **Okhuma, S., and B. Poole.** 1978. Fluorescence probe measurements of the intralysosomal pH in living cells and the perturbation of pH by various agents. Proc. Natl. Acad. Sci. USA **75:**3327–3331.
31. **Olsen, J., G. M. Cowell, E. Kønigshøfer, E. M. Danielsen, J. Møller, L. Laustsen, O. Hansen, K. G. Welinder, J. Engberg, W. Hunziker, M. Spiess, H. Sjöström, and O. Norén.** 1988. Complete amino acid sequence of human intestinal aminopeptidase N as deduced from cloned cDNA. FEBS Lett. **238:**307–314.
32. **Pensaert, M., P. Callebaut, and E. Cox.** 1993. Enteric coronaviruses of animals, p. 627–696. *In* A. Z. Kapikian (ed.), Viral infections of the gastrointestinal tract, 2nd ed. Marcel Dekker, New York, N.Y.
33. **Rasschaert, D., M. Duarte, and H. Laude.** 1990. Porcine respiratory coronavirus differs from transmissible gastroenteritis virus by a few genomic deletions. J. Gen. Virol. **71:**2599–2607.
34. **Rossen, J. W. A., C. P. J. Bekker, W. F. Voorhout, G. J. A. M. Strous, A. Van der Ende, and P. J. M. Rottier.** 1994. Entry and release of transmissible gastroenteritis coronavirus are restricted to apical surfaces of polarized epithelial cells. J. Virol. **68:**7966–7973.
35. **Sawicki, S. G., and D. Sawicki.** 1986. Coronavirus minus strand RNA synthesis and effect of cycloheximide on coronavirus RNA synthesis. J. Virol. **57:**328–334.
36. **Sjöström, H., and O. Norén.** 1982. Changes of the quaternary structure of microvillus aminopeptidase in the membrane. Eur. J. Biochem. **122:**245–250.
37. **Sturman, L. S., S. Richard, and K. V. Holmes.** 1990. Conformational changes of the coronavirus peplomer glycoprotein at pH 8.0 and 37°C correlates with virus aggregation and virus-induced cell fusion. J. Virol. **64:**3042–3050.
38. **Tresnan, D. B., R. Levis, and K. V. Holmes.** 1996. Feline aminopeptidase N serves as a receptor for feline, canaine, porcine, and human coronaviruses in serogroup I. J. Virol. **70:**8669–8674.
39. **Vogel, L. K., M. Spiess, H. Sjöström, and O. Norén.** 1992. Evidence for an apical sorting signal on the ectodomain of human aminopeptidase N. J. Biol. Chem. **267:**2794–2797.
40. **Vogel, L. K., O. Norén, and H. Sjöström.** 1995. Transcytosis of aminopeptidase N in Caco-2 cells is mediated by a non-cytoplasmic signal J. Biol. Chem. **270:**22933–22938.
41. **Wessels, H. P., G. H. Hansen, C. Fuhrer, A. T. Look, H. Sjöström, O. Norén, and M. Spiess.** 1990. Aminopeptidase N is directly sorted to the apical domain in MDCK cells. J. Cell Biol. **111:**2923–2930.
42. **Yeager, C. L., R. A. Ashmun, R. K. Williams, C. B. Cardellichio, L. H. Shapiro, A. T. Look, and K. V. Holmes.** 1992. Human aminopeptidase N is a receptor for human coronavirus 229E. Nature **357:**420–422.
43. **Yokomori, K. Y., and M. M. C. Lai.** 1992. Mouse hepatitis virus utilizes two carcinoembryonic antigens as alternative receptors. J. Virol. **66:**6194–6199.